Radiology: Artificial Intelligence

ORIGINAL RESEARCH

Accelerated Brain Aging in Amnestic Mild Cognitive Impairment: Relationships with Individual Cognitive Decline, Risk Factors for Alzheimer Disease, and Clinical Progression

Weijie Huang, BS • Xin Li, PhD • He Li, PhD • Wenxiao Wang, MS • Kewei Chen, PhD • Kai Xu, PhD • Junying Zhang, MS • Yaojing Chen, PhD • Dongfeng Wei, PhD • Ni Shu, PhD • Zhanjun Zhang, PhD

From the State Key Laboratory of Cognitive Neuroscience and Learning, Beijing Normal University, Beijing 100875, P. R. China (W.H., X.L., H.L., W.W., K.X., J.Z., Y.C., D.W., N.S., Z.Z.); Beijing Aging Brain Rejuvenation Initiative Centre, Beijing Normal University, Beijing, P. R. China (W.H., X.L., H.L., W.W., K.C., K.X., J.Z., Y.C., D.W., N.S., Z.Z.); Institute of Basic Research in Clinical Medicine, China Academy of Traditional Chinese Medicine, Beijing, P. R. China (H.L., J.Z., D.W.); and Banner Alzheimer's Institute, Phoenix, Ariz (K.C.). Received July 19, 2020; revision requested August 21; revision received May 6, 2021; accepted June 7. **Address correspondence to** N.S. (e-mail: *nshu@bnu.edu.cn*).

Supported by the National Natural Science Foundation of China (grant nos. 81471732, 81671761, and 81871425); National Science Fund for Distinguished Young Scholars (grant no. 81625025); Funds for International Cooperation and Exchange of the National Natural Science Foundation of China (grant no. 81820108034); National Key Research and Development Project of China (grant no. 2018YFC1315200); State Key Program of National Natural Science of China (grant no. 81430100); and Fundamental Research Funds for the Central Universities (grant no. 2017XTCX04).

Conflicts of interest are listed at the end of this article.

Radiology: Artificial Intelligence 2021; 3(5):e200171 • https://doi.org/10.1148/ryai.2021200171 • Content codes: AI MR NR

Purpose: To determine whether a brain age prediction model could quantify individual deviations from a healthy brain-aging trajectory (predicted age difference [PAD]) in patients with amnestic mild cognitive impairment (aMCI) and to determine if PAD was associated with individual cognitive impairment.

Materials and Methods: In this retrospective study, a machine learning approach was trained to determine brain age based on T1-weighted MRI scans. Two datasets were used for model training and testing—the Beijing Aging Brain Rejuvenation Initiative (BABRI) (616 healthy controls and 80 patients with aMCI, 2010–2018) and the Alzheimer's Disease Neuroimaging Initiative (ADNI) (589 healthy controls and 144 patients with aMCI, 2010–2018). A total of 974 healthy controls were used for model training (490 from BABRI and 484 from ADNI; age range, 49–95 years). The trained model was then tested on both healthy controls (126 from BABRI and 105 from ADNI) and patients with aMCI (80 from BABRI and 144 from ADNI) to estimate PAD (predicted age – actual age). Furthermore, the associations between PAD with cognitive impairment, genetic risk factors and pathologic markers of Alzheimer disease (AD), and clinical progression in patients with aMCI were examined using a partial correlation analysis, a two-way analysis of covariance, and a general linear model, respectively.

Results: Based on the prediction model, patients with aMCI were found to have higher PADs than those of healthy controls (BABRI: 2.65 ± 4.91 [standard deviation] vs 0.18 ± 4.79 [$P < .001$]; ADNI: 1.68 ± 5.28 vs 0.05 ± 4.41 [$P < .001$]). Moreover, the PAD was significantly associated with individual cognitive impairment in several cognitive domains in patients with aMCI ($P < .05$, corrected). When considering different AD-related risk factors, apolipoprotein E ε4 allele carriers were observed to have higher PADs than noncarriers (3.76 ± 4.82 vs 0.10 ± 5.05; $P = .017$), and patients with amyloid-positive aMCI were observed to have higher PADs than patients with amyloid-negative status (2.40 ± 5.25 vs 0.93 ± 5.20; $P = .003$). Finally, PAD combined with other markers of AD at baseline for differentiating between progressive and stable aMCI resulted in an area under the curve value of 0.87.

Conclusion: The PAD is a sensitive imaging marker related to individual cognitive differences in patients with aMCI.

Supplemental material is available for this article.

As a transitional phase from normal aging to Alzheimer disease (AD), amnestic mild cognitive impairment (aMCI) involves episodic memory loss isolated from or associated with other forms of cognitive decline (1). With advanced neuroimaging techniques, aging-related trajectories of brain structures and functions have been observed in patients with aMCI that are distinct from those in healthy older individuals (2,3), suggesting a deviation from the typical brain-aging trajectory in aMCI. However, there is heterogeneity in the clinical manifestations and progression to dementia in patients with aMCI (4). Understanding the individual deviations from the typical brain-aging trajectory in aMCI is important for the early identification of and intervention for patients at high risk of developing AD.

To quantify the deviation from the typical brain-aging trajectory, brain-based age prediction offers a promising approach for providing personalized markers of future cognitive impairments (5,6). Brain age is estimated by an age prediction model trained on a large sample of the healthy population with neuroimaging data (7,8). Establishing the typical trajectory of brain aging in healthy older individuals provides a basis for characterizing clinically relevant deviations. Using this approach, accelerated brain aging was found in patients with AD (9), traumatic brain injury (10), human immunodeficiency virus (11), and schizophrenia (12). Importantly, the predicted age difference (PAD) (predicted age – chronologic age) could potentially

Abbreviations

AD = Alzheimer disease, ADNI = Alzheimer's Disease Neuroimaging Initiative, aMCI = amnestic mild cognitive impairment, APOE = apolipoprotein E, BABRI = Beijing Aging Brain Rejuvenation Initiative, MMSE = Mini-Mental State Examination, PAD = predicted age difference, SUVR = standardized uptake value ratio

Summary

A model was developed to predict brain age to quantify individual deviations from the typical brain-aging trajectory in amnestic mild cognitive impairment.

Key Points

- The predicted age difference (PAD) (predicted age – actual age) was associated with individual measures of cognitive impairment measured in patients (from two different datasets) with amnestic mild cognitive impairment (aMCI) in several domains, specifically including memory ($r = -0.33$, $P = .005$ and $r = -0.34$, $P < .001$), attention (assessed in only one dataset, $r = -0.40$, $P < .001$), and executive function (significant in only one dataset $r = -0.26$, $P = .002$).
- In patients with aMCI, apolipoprotein E (APOE) ε4 carriers had higher PADs than noncarriers (3.76 ± 4.82 vs 0.10 ± 5.05; $P = .017$) and patients with amyloid-positive disease had higher PADs compared with those with amyloid-negative disease (2.40 ± 5.25 vs 0.93 ± 5.20; $P = .003$).
- Combining the PAD with other markers of Alzheimer disease (APOE carrier status, amyloid status, and Mini-Mental State Examination) showed the highest performance in differentiating progressive aMCI from stable aMCI, with an area under the curve value of 0.87.

Keywords

MR Imaging, Brain/Brain Stem, Brain Age, Machine Learning, Mild Cognitive Impairment, Structural MRI

depict the extent of the deviation from healthy brain-aging trajectories (5), which was shown to be sensitive to cognitive impairment (9,13–15) and the incidence of dementia (16). Some previous studies have found that the brain-aging trajectory is related to cognitive impairments and that apolipoprotein E (APOE) ε4 and amyloid β have an effect on the trajectory across the spectrum of AD (9,15,17). To our knowledge, however, no study has systematically explored the individual differences in the brain-aging trajectory of patients with aMCI.

Here, we aimed to explore whether PAD could quantify individual deviations from the typical brain-aging trajectory in patients with aMCI. We began by training a brain age prediction model based on two imaging cohorts consisting of individuals with normal cognition aged 49 to 95 years old, and then we used this model to test the following hypotheses: *(a)* if patients with aMCI have higher PADs than those of healthy older individuals, *(b)* if PAD is associated with individual cognitive decline in patients with aMCI, *(c)* if different risk factors for AD have an effect on the PAD in patients with aMCI, and *(d)* if combining PAD with disease-specific markers at baseline would improve the prediction accuracy of clinical progression in aMCI.

Materials and Methods

Patients

This retrospective study was approved by the ethics committee of the institutional review board of the Beijing Normal University Imaging Center for Brain Research. Two independent patient samples were included in the present study—the Beijing Aging Brain Rejuvenation Initiative (BABRI) and the Alzheimer's Disease Neuroimaging Initiative (ADNI) datasets (*http://adni.loni.usc.edu*). The healthy controls in BABRI were used to explore the relationship between structural connectivity degeneration and cognitive decline with normal aging in our previous study (19). Detailed descriptions of the samples from the two datasets are provided as follows.

BABRI dataset.— The present sample consisted of 616 healthy controls and 80 patients with aMCI who were right-handed and native Chinese speakers recruited from 2010 to 2018 from the BABRI project, an ongoing longitudinal study in Beijing, China. Diagnosis of aMCI was according to Petersen criteria (20) as follows: *(a)* subjective memory complaints, *(b)* a score of 24 or higher on the Chinese version of the Mini-Mental State Examination (MMSE), *(c)* intact activities of daily living and instrumental activities of daily living, *(d)* no dementia, and *(e)* cognitive impairments in memory. The criteria for healthy controls were as follows: *(a)* no cognitive complaints, *(b)* normal cognitive ability, and *(c)* intact activities of daily living and instrumental activities of daily living. The exclusion criteria were as follows: *(a)* the presence of structural abnormalities other than cerebrovascular lesions (tumors, subdural hematomas, and contusions owing to previous head trauma that could impair cognitive function); *(b)* a history of addictions, neurologic or psychiatric disease, or treatments that would affect cognitive function; *(c)* large vessel disease, such as cortical or subcortical infarcts and watershed infarcts; and *(d)* diseases with white matter lesions, such as normal pressure hydrocephalus and multiple sclerosis. All participants underwent comprehensive neuropsychologic testing and MRI scanning. Each participant provided written informed consent.

ADNI dataset.— This study included 589 right-handed healthy controls and 144 patients with aMCI recruited from 2010 to 2018 from the ADNI dataset (ie, ADNI-GO, ADNI-2, and ADNI-3). In the present study, all participants had T1-weighted MRI data. For all patients with aMCI, their APOE genotype had been documented and amyloid fluorine 18 (^{18}F)-florbetapir PET acquisition data were available. Among these patients, 56 had up to 5 years of follow-up clinical data. General criteria for categorizing healthy controls and patients with aMCI are explained in the clinical protocols of the ADNI dataset (*http://adni.loni.usc.edu/methods/documents/*). Up-to-date information is available at *www.adni-info.org*.

Neuropsychologic Testing

For the BABRI dataset, all participants underwent a multitude of neuropsychologic tests assessing their general mental status

Table 1: Demographic Characteristics of Training Healthy Control Datasets

Characteristic	BABRI	ADNI
No. of individuals	490	484
Age (y)	66 ± 7 (49–85)	73.9 ± 6.7 (55.8–95.4)
Sex		
No. of men	190	197
No. of women	300	287
Education (y)	11.7 ± 3.2 (0–23)	16.7 ± 2.4 (11–20)
MMSE	28.0 ± 1.6 (24–30)	29.0 ± 1.2 (24–30)

Note.—Continuous variables shown as mean ± standard deviation, with range in parentheses. ADNI = Alzheimer's Disease Neuroimaging Initiative, BABRI = Beijing Aging Brain Rejuvenation Initiative, MMSE = Mini-Mental State Examination.

(MMSE) and function in five cognitive domains, including memory, attention, executive function, language, and visuospatial ability. For the ADNI dataset, the MMSE was used to assess general mental status. The ADNI-memory and ADNI-executive function scores were used as cognitive domain measurements (18). Detailed descriptions of neuropsychologic tests in both datasets are provided in Appendix E1 (supplement).

Image Acquisition

BABRI dataset.— The BABRI MRI dataset was acquired with a 3-T MRI scanner (Trio, Siemens Healthineers) in the Imaging Center for Brain Research at Beijing Normal University. High-resolution T1-weighted imaging covering the whole brain was performed using sagittal three-dimensional magnetization-prepared rapid gradient-echo sequences. The acquisition parameters were as follows: repetition time msec/echo time msec/inversion time msec, 1900/3.44/900; section thickness, 1 mm; no intersection gap; 176 axial sections; matrix size, 256 × 256; field of view, 256 × 256 mm^2; flip angle, 9°; and voxel size, 1 × 1 × 1 mm^3.

ADNI dataset.— High-resolution three-dimensional T1-weighted MRI was performed with 3.0-T scanners (GE Healthcare) at multiple centers using accelerated sagittal magnetization-prepared rapid gradient-echo sequences (2300/2.98/900; section thickness, 1 mm; no intersection gap; 176 axial sections; matrix size, 240 × 256; field of view, 240 × 256 mm^2; flip angle, 9°; and voxel size, 1 × 1 × 1 mm^3) and inversion recovery fast spoiled gradient-echo sequences (echo time msec/inversion time msec, 3.1/400; section thickness, 1 mm; no intersection gap; 196 axial sections; matrix size, 256 × 256; field of view, 256 × 256 mm^2; flip angle, 11°; and voxel size, 1 × 1 × 1 mm^3). Additionally, ^{18}F-florbetapir PET data were acquired 50–70 minutes after injection. For the detailed scanning parameters, see Jack et al (21) or *www.adni-info.org*.

Image Processing

For the T1-weighted image, a gray matter volume map in Montreal Neurological Institute space was generated for each individual using the CAT12 toolbox (*http://www.neuro.uni-jena.de/cat/*). Hippocampal volume was calculated with the sum of the values of the gray matter volume map in the hippocampal region, which was defined by the automated anatomic labeling atlas (22). To calculate the cortical standardized uptake value ratio (SUVR) from PET images, we normalized the averaged standardized uptake value from the prefrontal, orbitofrontal, parietal, temporal, anterior cingulate, and posterior cingulate regions with the mean uptake in the cerebellar crus regions (23–26). Finally, participants were classified as amyloid-positive or amyloid-negative based on a threshold of 1.36, which was the median value of all individuals' SUVR values. Detailed descriptions of the processing procedure are provided in Appendix E2 (supplement).

Brain Age Prediction

To construct a brain age prediction model, approximately four-fifths of healthy control samples in the BABRI (n = 490) and ADNI (n = 484) datasets were selected as the training dataset (Table 1), with a simple random sampling. The other one-fifth of the healthy controls (BABRI: n = 126; ADNI: n = 105) in the two datasets were used as the test dataset. In addition, all patients with aMCI in the two datasets were used as a test dataset to evaluate whether the brain age prediction model could quantify individual deviations from the typical brain-aging trajectory in patients with aMCI. The pipeline for brain age prediction consisted of the following four steps: *(a)* feature extraction, *(b)* model construction, *(c)* model evaluation, and *(d)* brain age prediction (Fig 1). A detailed description of each step follows.

Feature extraction.— For each participant, we extracted intensity values from the gray matter volume map and converted them into a row vector, each element of which represented the intensity value of a voxel. Then, all vectors from each individual were concatenated into a feature matrix. Before these features were normalized, the features for which standard deviations among the training dataset were equal to zero were removed. Finally, the mean values and standard deviations of the features in the training dataset were used to normalize the feature values for all individuals.

Model construction.— We trained the elastic net model with two hyperparameters to predict age. These two hyperparameters include α, which controls the amount of shrinkage of a model's parameter, and λ, which controls the relative weighting of the L1-norm and L2-norm contributions. To optimize the hyperparameters, three-fourths of the training dataset was used for training the models with different possible hyperparameters. Specifically, the α was set as $\alpha = e^{\gamma}$, where γ was chosen from 20 values in the range of [−6, 5] and λ was chosen from 10 values in the range of [0.2, 1.0] (27,28). Therefore, a total of 200 possible parameter sets (α, λ) were obtained. For each set of hyperparameters, we trained the model on the

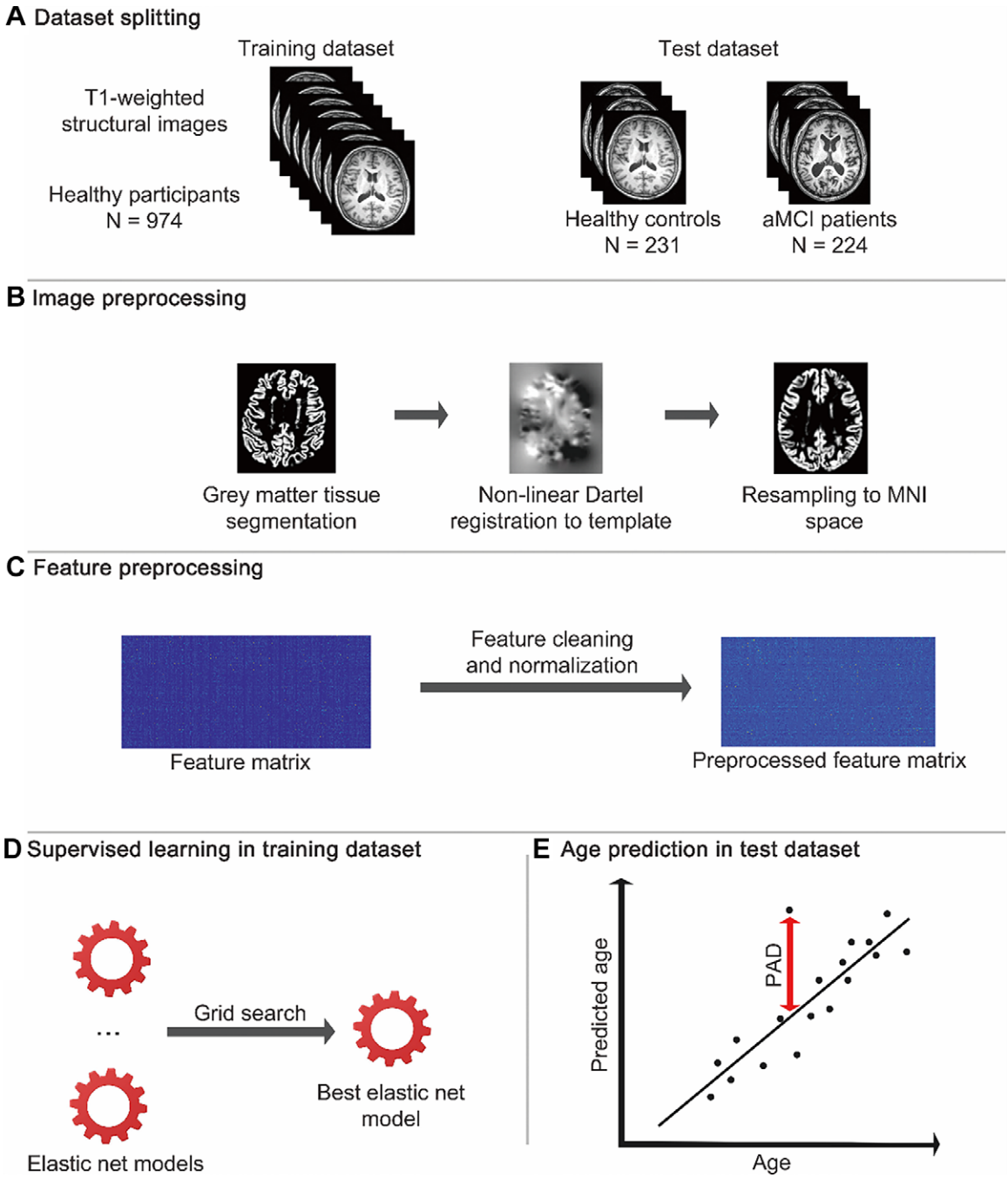

Figure 1: Flowchart shows framework of brain age prediction model. **(A)** Imaging data were split into training and test datasets. Training dataset consisted of structural MRI data from 974 healthy individuals, whereas test dataset included data from two groups—231 healthy controls and 224 patients with amnestic mild cognitive impairment (aMCI). **(B)** Conventional statistical parametric mapping structural preprocessing pipeline was used to generate gray matter volume maps in Montreal Neurological Institute (MNI) space. Dartel = diffeomorphic anatomic registration through exponentiated lie algebra. **(C)** Intensity values from gray matter volume maps were extracted and concatenated to create feature matrix that was then cleaned and normalized. **(D)** The best elastic net model was obtained by performing supervised learning on training dataset. To optimize hyperparameters, grid search was performed. **(E)** Test dataset was input into trained model. Age was predicted for every patient included in test dataset. Predicted age difference (PAD) scores were calculated by subtracting patient's chronologic age from his or her predicted age.

three-fourths of the training dataset and evaluated the model performance on the remaining one-fourth of the training dataset. The best model was selected with the highest Pearson correlation coefficient between actual age and predicted age according to the calculation using the one-fourth left-out partition of the training data. To evaluate the effects of different machine learning algorithms, we also applied the same pipeline to train two other types of linear regression models (ie, least absolute shrinkage and selection operator regression and ridge regression), support vector regression model, Gaussian process regression model, and convolutional neural network model with the same architecture as a previous study (29).

Model evaluation.— Model accuracy was assessed on the one-fifth test dataset using several measures, including the Pearson correlation coefficient, mean squared error, mean absolute error, and predicted R^2 (30), which has been suggested as an alternative to the statistical R^2 measure for assessing numeric accuracy in regressions.

Brain age prediction.— Finally, the test dataset was input into trained models. An age was predicted for every participant included in the test dataset. The PAD scores were calculated by subtracting the participant's chronologic age from his or her predicted age. The pipeline was carried out using Python software (version 3.8, *https://www.python.org/*), Python library scikit-learn (version 0.23.2, *https://scikit-learn.org/stable/*), and PyTorch (version 1.8.0, *https://pytorch.org/*).

Statistical Analysis

For the test samples, group differences in demographic characteristics and neuropsychologic scores between patients with aMCI and healthy controls were compared using two-sample *t* tests; the exception to this was sex, which was compared using the χ^2 test. To compare the PADs between the healthy control and aMCI groups, a general linear model or a Mann-Whitney test was carried out depending on whether the PADs of the healthy control and aMCI groups followed a normal distribution.

Partial correlation analyses with the Bonferroni correction were performed to explore the relationship between PADs and multiple cognitive scores in patients with aMCI. $P < .008$ (.05/6) and $< .017$ (.05/3) were considered statistically significant in the BABRI and ADNI datasets, respectively, because the BABRI dataset includes six cognitive scores and the ADNI dataset includes three cognitive scores. To evaluate how much of the variance of cognition could be explained by the PAD and the whole model, we constructed a general linear model in which cognitive scores were dependent variables and in which age, sex, years of education, and PAD were independent variables. Then we calculated R^2 to evaluate the proportion of the variance explained by the PAD (R^2_{PAD}) and the whole model (R^2_{model}), respectively (31). We also performed a linear mixed model to validate the relationship between PAD and cognition.

To assess the effect of amyloid and APOE $\varepsilon 4$ and their interaction on PAD in patients with aMCI, a two-way analysis of covariance was performed. Moreover, the partial correlation between the PAD and amyloid SUVR values was evaluated. Finally, a general linear model was used to compare the PADs between progressive and stable in patients with aMCI. To evaluate the ability of the PAD at baseline combined with other pathologic markers of AD to predict clinical progression in aMCI, we used a naive Bayesian classifier to classify progressive aMCI from stable aMCI with different feature sets and compared their performances with leave-one-out cross-validation. The significance of accuracy, sensitivity, and specificity were obtained by permutation tests. Age, sex, and years of education were regressed out as control variables.

All of the aforementioned statistical analyses were performed with R software (version 3.6.2, *https://www.r-project.org/*), R libraries relaimpo (version 2.2–3, *https://cran.r-project.org/web/packages/relaimpo/index.html*), and lme4 (version 1.1–23, *https://github.com/lme4/lme4/*).

Data Availability

The datasets generated and analyzed in the present study will be made available from the corresponding author to other scientists on request in anonymized format and according to data protection policy in the ethics agreement.

Results

Demographic and Neuropsychologic Characteristics

The training datasets consisted of 490 healthy controls (190 men) 49 to 85 years of age in the BABRI dataset and 484 healthy controls (197 men) 56 to 95 years of age in the ADNI dataset. The average years of education were 11.7 years ± 3.2 [standard deviation] and 16.7 years ± 2.4 in the BABRI and ADNI datasets, respectively. The MMSE scores were greater than 24 for all individuals within the training datasets (Table 1). For the test samples in the BABRI dataset, no group differences in age, sex, or years of education were found between patients with aMCI and healthy controls.

For neuropsychologic scores in the BABRI dataset, patients with aMCI had lower scores than did healthy controls on the MMSE (26.7 ± 1.8 vs 28.1 ± 1.5; $P < .001$) as well as on the memory (–1.02 ± 0.50 vs 0.30 ± 0.71; $P < .001$), executive function (–0.27 ± 0.79 vs 0.34 ± 0.52; $P < .001$), attention (–0.19 ± 0.73 vs 0.34 ± 0.60; $P < .001$), language (–0.48 ± 0.73 vs 0.28 ± 0.64; $P < .001$), and visuospatial ability (–0.25 ± 0.86 vs 0.28 ± 0.64; $P < .001$) assessments.

In the ADNI dataset, patients with aMCI and healthy controls had similar ages and years of education, but the aMCI group had a higher proportion of men than did the healthy control group (58.3% vs 41.0%; $P = .01$). For neuropsychologic scores, patients with aMCI scored lower than healthy controls on the MMSE (28.0 ± 1.7 vs 29.1 ± 1.3; $P < .001$) as well as on the memory (0.26 ± 0.61 vs 1.03 ± 0.53; $P < .001$) and executive function (0.21 ± 0.81 vs 0.94 ± 0.85; $P < .001$) assessments. Detailed descriptions of the demographic information and neuropsychologic performance of the test samples are provided in Table 2.

Prediction Performance of Different Machine Learning Methods

As expected, chronologic age could be accurately predicted from T1-weighted MRI scans. Of the models tested, the elastic net model achieved the highest performance in predicting the chronologic age of healthy controls in the test dataset (predicted chronologic age correlation $r = 0.872$, predicted $R^2 = 0.753$, mean squared error = 16.605, mean absolute error = 3.012 years). To evaluate the influence of different machine learning methods on the prediction results, we also compared the performance of five other models trained with different machine learning algorithms (Fig 2). Table 3 shows performance metrics for the other five models assessed. Moreover,

Table 2: Demographic Characteristics and Neuropsychologic Performance of the Test Population

	BABRI				ADNI			
Variable	HC (n = 126)	aMCI (n = 80)	P Value	T or F Statistic	HC (n = 105)	aMCI (n = 144)	P Value	T or F Statistic
Demographic information								
Age (y)	66 ± 8 (46–86)	67 ± 8 (54–86)	.71*	0.38*	73.4 ± 7.0 (56.2–91.4)	74.7 ± 7.6 (56.2–93.2)	.14*	−1.49*
Sex			.27†	1.20†			.01†	6.72†
Men	44	34			43	84		
Women	82	46			62	60		
Education (y)	11.9 ± 3.0 (6–18)	11.4 ± 3.4 (1–17)	.25*	−1.15*	16.5 ± 2.4 (12–20)	16.0 ± 2.8 (8–20)	.14*	1.47*
Cognition information								
MMSE	28.1 ± 1.5 (24–30)	26.7 ± 1.8 (24–30)	<.001*	−5.90*	29.1 ± 1.3 (24–30)	28.0 ± 1.7 (24–30)	<.001*	−5.72*
Memory	0.30 ± 0.71 (−1.19 to 2.42)	−1.02 ± 0.50 (−1.74 to 0.13)	<.001*	−15.33*	1.03 ± 0.53 (−0.22 to 2.21)	0.26 ± 0.61 (−1.30 to 2.28)	<.001*	−10.34
Executive function	0.34 ± 0.52 (−1.27 to 1.69)	−0.27 ± 0.79 (−2.87 to 1.21)	<.001*	−6.00*	0.94 ± 0.85 (−1.10 to 2.99)	0.21 ± 0.81 (−2.23 to 2.25)	<.001*	−6.62
Attention	0.34 ± 0.60 (−1.78 to 2.43)	−0.19 ± 0.73 (−2.29 to 1.31)	<.001*	−5.33*	NA	NA	NA	NA
Language	0.28 ± 0.64 (−1.43 to 1.73)	−0.48 ± 0.73 (−2.10 to 1.80)	<.001*	−7.58*	NA	NA	NA	NA
Visuospatial function	0.28 ± 0.64 (−1.43 to 1.73)	−0.25 ± 0.86 (−4.77 to 0.78)	<.001*	−3.95*	NA	NA	NA	NA

Note.—Continuous variables shown as mean ± standard deviation, with range in parentheses. ADNI = Alzheimer's Disease Neuroimaging Initiative, aMCI = amnestic mild cognitive impairment, BABRI = Beijing Aging Brain Rejuvenation Initiative, HC = healthy control, MMSE = Mini-Mental State Examination, NA = not available.
* The P values were obtained by using two-sample t tests, with T statistic shown.
† The P values were obtained by using χ^2 tests, with F statistic shown.

the prediction accuracies in terms of mean absolute error in our models were comparable with those obtained from other studies (9,10,12–17,32) with similar brain age prediction frameworks (Table E1 [supplement]).

To explore which brain regions contributed to brain age predictions, we selected the gray matter voxels with a nonzero regression coefficient in the trained elastic net model. As shown in Table E2 (supplement), the medial temporal cortex, superior frontal cortex, and some subcortical nuclei played important roles in brain age prediction.

Predicted Brain Age Correlates with Individual Cognitive Impairment of Patients with aMCI

For each test sample, a PAD score was obtained according to the trained elastic net model. Compared with healthy controls, patients with aMCI from both the BABRI and ADNI datasets showed higher PADs (BABRI: 2.65 ± 4.91 vs 0.18 ± 4.79 [$P < .001$]; ADNI: 1.68 ± 5.28 vs 0.05 ± 4.41 [$P < .001$]) (Fig 3A). Furthermore, in the BABRI dataset, PAD was associated with memory ($r = -0.33$, $P = .005$), attention ($r = -0.40$, $P < .001$), and language ($r = -0.33$, $P = .004$) (Fig 3B).

In the ADNI dataset, PAD was also correlated with memory ($r = -0.34$, $P < .001$), executive function ($r = -0.26$, $P = .002$), and MMSE ($r = -0.32$, $P < .001$) scores in patients with aMCI (Fig 3C). When removing two outliers with PAD of greater than 15, the results remained largely unchanged. However, no such correlation between PADs and cognitive scores was observed in healthy control groups in either the BABRI or ADNI datasets (Table 4). To validate the result, a linear mixed model was performed; the correlation results remained largely unchanged (Table E3 [supplement]). All R^2_{PAD} and R^2_{model} values are shown in Table 4.

We also compared the PAD values between healthy controls and all patients with MCI (n = 175) in the BABRI dataset, including both aMCI (n = 80) and nonamnestic MCI (n = 95) groups. Similarly, the patients with MCI had higher PADs than did the healthy controls (1.60 ± 5.06 vs 0.18 ± 4.79, $P < .001$). Moreover, the PAD was correlated with executive function score ($r = -0.25$, $P = .003$), attention score ($r = -0.25$, $P = .002$), and language score ($r = -0.29$, $P = .001$) but not with memory score ($r = -0.16$, $P = .055$), across all patients with MCI (nonamnestic and amnestic) (Fig E1 [supplement]). All R^2_{PAD} and R^2_{model} values are

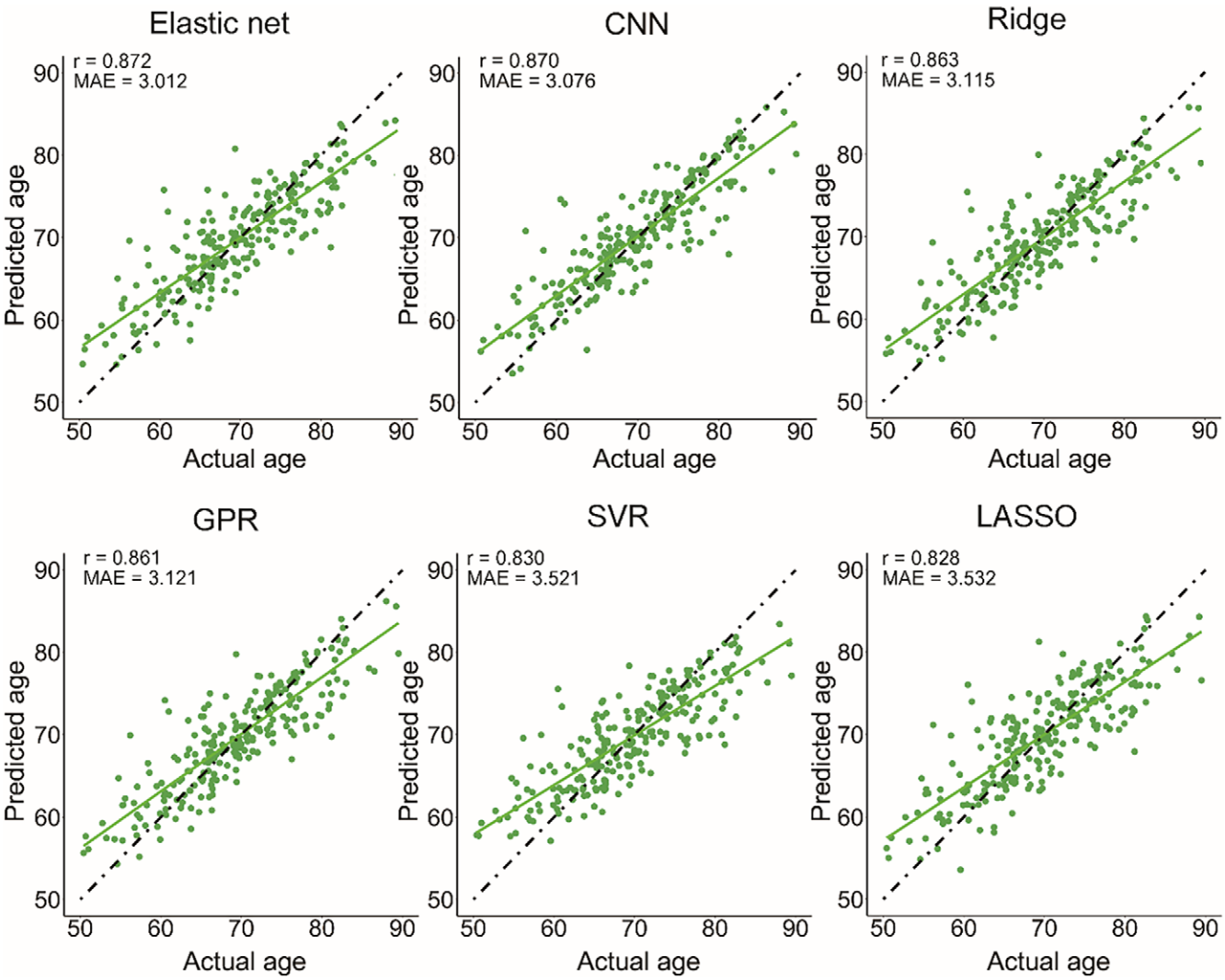

Figure 2: Performance of different machine learning approaches in predicting chronologic age of healthy controls in test dataset. Scatterplots show actual age and brain age predicted with different machine learning methods. CNN = convolutional neural network, GPR = Gaussian process regression, LASSO = least absolute shrinkage and selection operator, MAE = mean absolute error, SVR = support vector regression.

Table 3: Performance of Different Machine Learning Algorithms

Algorithm	Predicted Chronologic Age Correlation	Predicted R^2	MSE	MAE (y)
LASSO regression	0.828	0.682	21.3	3.5
SVR	0.830	0.674	21.9	3.5
GPR	0.861	0.734	17.9	3.1
Ridge regression	0.863	0.739	17.6	3.1
CNN	0.870	0.753	16.6	3.0
Elastic net model	0.872	0.753	16.6	3.0

Note.—CNN = convolutional neural network, GPR = Gaussian process regression, LASSO = least absolute shrinkage and selection operator, MAE = mean absolute error, MSE = mean squared error, SVR = support vector regression.

shown in Table E4 (supplement). The demographic characteristics and neuropsychologic performance of all patients with amnestic and nonamnestic MCI are presented in Table E5 (supplement).

Effects of AD Risk Factors on the Predicted Brain Age of Patients with aMCI

For amyloid status, the patients with aMCI from the ADNI dataset were classified into 71 amyloid-negative and 73 amyloid-positive patients with a SUVR threshold of 1.36. When considering APOE genotypes, there were 62 APOE ε4 carriers and 82 noncarriers. Detailed descriptions of the demographic characteristics and neuropsychologic performance of the aMCI subgroups are provided in Table 5.

Two-way analysis of covariance revealed significant main effects of amyloid deposition (F = 9.45, P = .003) and APOE ε4 (F = 5.82, P = .017) on the PADs of patients with aMCI (Fig 4), suggesting that APOE ε4 carriers exhibited higher PADs than those of noncarriers

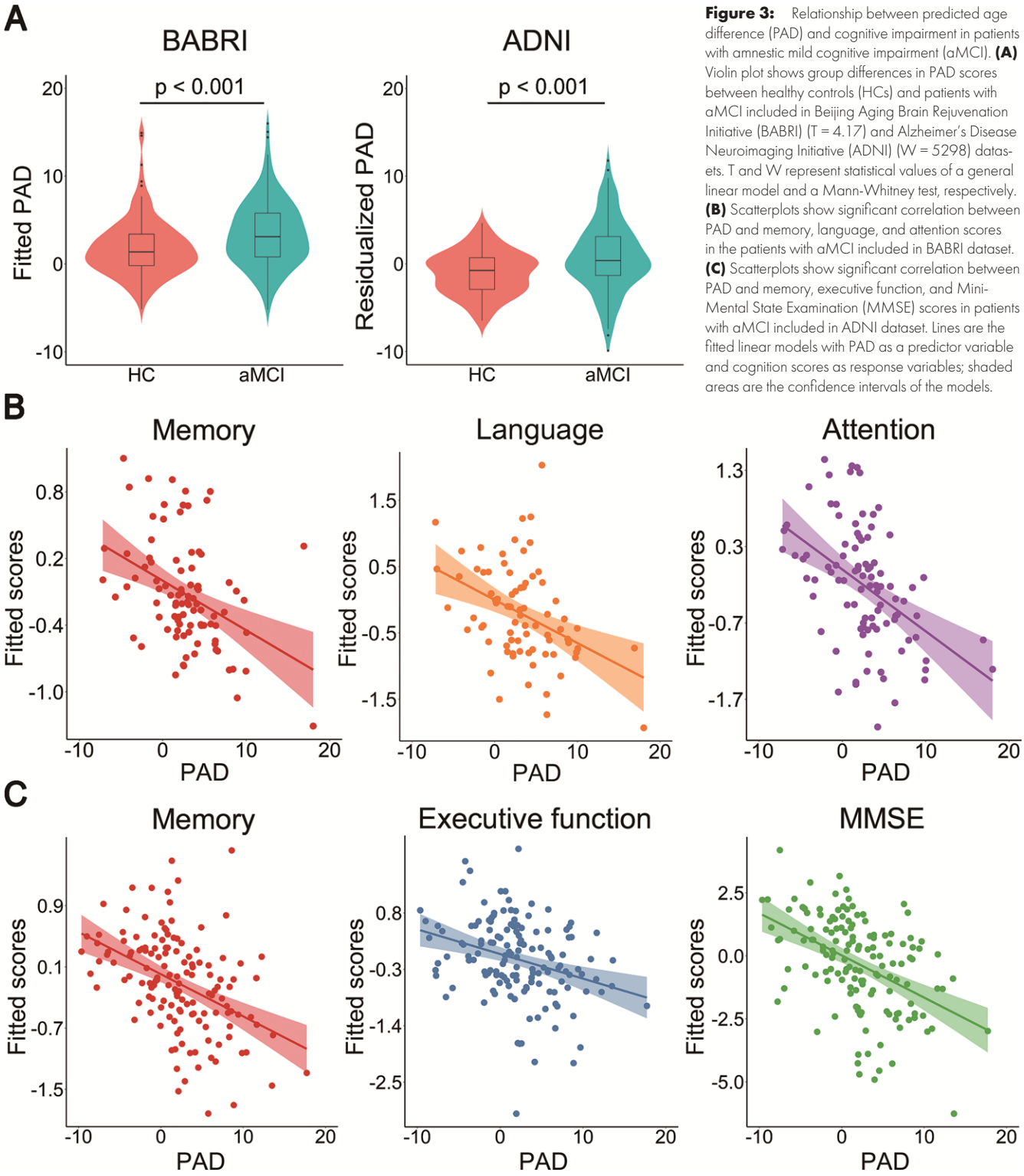

Figure 3: Relationship between predicted age difference (PAD) and cognitive impairment in patients with amnestic mild cognitive impairment (aMCI). **(A)** Violin plot shows group differences in PAD scores between healthy controls (HCs) and patients with aMCI included in Beijing Aging Brain Rejuvenation Initiative (BABRI) (T = 4.17) and Alzheimer's Disease Neuroimaging Initiative (ADNI) (W = 5298) datasets. T and W represent statistical values of a general linear model and a Mann-Whitney test, respectively. **(B)** Scatterplots show significant correlation between PAD and memory, language, and attention scores in the patients with aMCI included in BABRI dataset. **(C)** Scatterplots show significant correlation between PAD and memory, executive function, and Mini-Mental State Examination (MMSE) scores in patients with aMCI included in ADNI dataset. Lines are the fitted linear models with PAD as a predictor variable and cognition scores as response variables; shaded areas are the confidence intervals of the models.

and that amyloid-positive patients with aMCI exhibited higher PADs than those of amyloid-negative patients. No interaction was found between amyloid and APOE ε4 regarding PAD (F = 0, P = .996). When treating amyloid SUVR as a continuous variable, the results showed a significant correlation between the amyloid SUVR and PAD score across patients with aMCI (r = 0.17, P = .046).

Brain Age Predicts the Clinical Progression of Patients with aMCI

During longitudinal follow-up for up to 5 years (n = 56 patients), 33 patients with aMCI progressed to AD and 23 remained stable. No group differences in baseline demographic data, including age, sex, and years of education, were found between the progressive and stable aMCI groups. Based on the baseline T1-weighted im-

Table 4: Pearson Correlation between Cognition and PAD in Healthy Control and aMCI Groups

	Healthy Control		aMCI			
Variable	*r* Value	*P* Value	*r* Value	*P* Value	R^2_{PAD} (%)	R^2_{model} (%)
BABRI						
Memory	0.07	.43	−0.33	.005*	4.47	23.10
Executive function	−0.13	.16	−0.28	.016	NA	NA
Attention	−0.06	.51	−0.40	<.001*	8.57	24.63
Language	0.16	.009	−0.33	.004*	5.68	17.97
Visuospatial function	0	>.99	−0.03	.76	NA	NA
MMSE	−0.17	.06	−0.12	.29	NA	NA
ADNI						
Memory	−0.10	.33	−0.34	<.001*	8.19	15.69
Executive function	0.06	.58	−0.26	.002*	3.06	16.19
MMSE	0.08	.43	−0.32	<.001*	6.01	14.48

Note.—ADNI = Alzheimer's Disease Neuroimaging Initiative, aMCI = amnestic mild cognitive impairment, BABRI = Beijing Aging Brain Rejuvenation Initiative, MMSE = Mini-Mental State Examination, NA = not available, PAD = predicted age difference.
* *P* values are significant.

Table 5: Demographic Characteristics and Neuropsychologic Performance of aMCI Subgroups in ADNI Dataset

Variable	APOE ε4−, Amyloid− (*n* = 54)	APOE ε4−, Amyloid+ (*n* = 28)	APOE ε4+, Amyloid− (*n* = 17)	APOE ε4+, Amyloid+ (*n* = 45)	*P* Value	F Statistic
Age (y)	74.9 ± 7.2 (61.8–91.6)	80.1 ± 5.4 (71.0–93.2)	69.0 ± 8.4 (56.2–84.1)	73.2 ± 6.6 (56.5–86.3)	<.001	10.34
Sex					.43	2.74
Men	30	15	13	26		
Women	24	13	4	19		
Education (y)	16.2 ± 2.5 (8–20)	16.3 ± 3.0 (11–20)	16.3 ± 3.5 (8–20)	15.3 ± 2.6 (11–20)	.32	1.18
MMSE	28.6 ± 1.4 (25–30)	27.6 ± 1.4 (25–30)	27.9 ± 1.9 (24–30)	27.5 ± 1.8 (24–30)	.006	4.37
Memory	0.48 ± 0.58 (−0.53 to 2.28)	0.35 ± 0.58 (−0.59 to 1.80)	0.21 ± 0.53 (−1.17 to 1.06)	−0.06 ± 0.56 (−1.30 to 0.99)	.001	7.54
Executive function	0.47 ± 0.85 (−2.23 to 2.25)	0.13 ± 0.74 (−1.41 to 2.23)	0.08 ± 0.71 (−1.17 to 1.42)	−0.01 ± 0.73 (−1.64 to 1.28)	.02	3.38

Note.—Continuous variables shown as mean ± standard deviation, with range in parentheses. Differences among the four groups were compared with analysis of variance or χ^2 tests as appropriate. Amyloid− = amyloid-negative patients, Amyloid+ = amyloid-positive patients, APOE = apolipoprotein E, APOE4− = APOE ε4 noncarriers, APOE4+ = APOE ε4 carriers, MMSE = Mini-Mental State Examination.

age, PAD scores were calculated for both groups. The progressive aMCI group had a higher baseline PAD than did the stable aMCI group (4.83 ± 4.70 vs 0.40 ± 4.81, $P < .001$) (Fig 5A). The performance of different combinations of AD-related features in differentiating progressive aMCI and stable aMCI is shown in Table 6. PAD at baseline combined with the MMSE score, amyloid SUVR values, and APOE ε4 genotype had an area under the curve value of 0.87 for differentiating between stable and progressive aMCI (Fig 5B).

Discussion

This study included a large sample of middle-aged and older adults from multiple centers that was used to develop a machine learning model for brain age prediction according to MRI-derived gray matter tissue volume. We found that patients with aMCI had brain aging trajectories that were distinct from aging trajectories in healthy individuals. We used the developed model to predict brain age of patients with aMCI and then assessed if there were associations with risk factors for cognitive decline. The individual differences in brain aging were modulated with the APOE ε4 genotype and amyloid β level. Finally, we found that patients with progressive aMCI exhibited more deviations from typical normal aging than did patients with stable aMCI, and the use of the PAD score along with other AD-specific markers had higher performance for predicting the progression of aMCI.

On the basis of the T1-weighted MR images, we constructed six models to predict individual age and compared their performance. The six models predicted age accurately; however, the elastic net model slightly outperformed other methods, likely because this method consists of a combination of the other methods tested (ie, ridge and least absolute shrinkage and selection operator regression). Therefore, we chose the elastic net model for the subsequent analyses because of its higher performance and interpretability. The elastic net model is a sparse model that during training adjusts to zero the weight of features that contribute little to predicting age. The remaining features with weights greater than zero were located in the temporal and frontal lobes and some subcortical nuclei, which atrophy with aging (33–35). Specifically, atrophy of the parahippocampal gyrus, hippocampus, middle temporal gyrus, and medial superior frontal gyrus was more prevalent in patients with AD or with aMCI (36,37).

Our results and those of previous studies (9,10,12–17,29) indicated that the choice of machine learning models may not have a considerable effect on the accuracy of predicting the chronologic age; however, the training dataset is important. Compared with the previous studies, ours had a relatively large training dataset and included only geriatric data. Our model had higher performance than other studies that used young and middle-aged participants for model training. However, younger and middle-aged populations have different brain-aging trajectories than older adults. These trajectories can be difficult to model, which may explain why these models have lower performance.

The predictive model we generated was highly accurate at estimating chronologic age in healthy participants based only on the appearance of T1-weighted MRI scans. In contrast, for aMCI, the model estimated brain age to be greater than 2.7 years older on average than the patient's chronologic age. This discrepancy was independent of the aging and was not observed in healthy controls, whose predicted brain age was 0.2 years older on average than their chronologic age, which supports the theory proposed by Driscoll et al (38) that aMCI may hasten the aging process and is consistent with long-term structural brain abnormalities reported in neuroimaging and neuropathology studies in patients with aMCI. Nevertheless, the degree to which

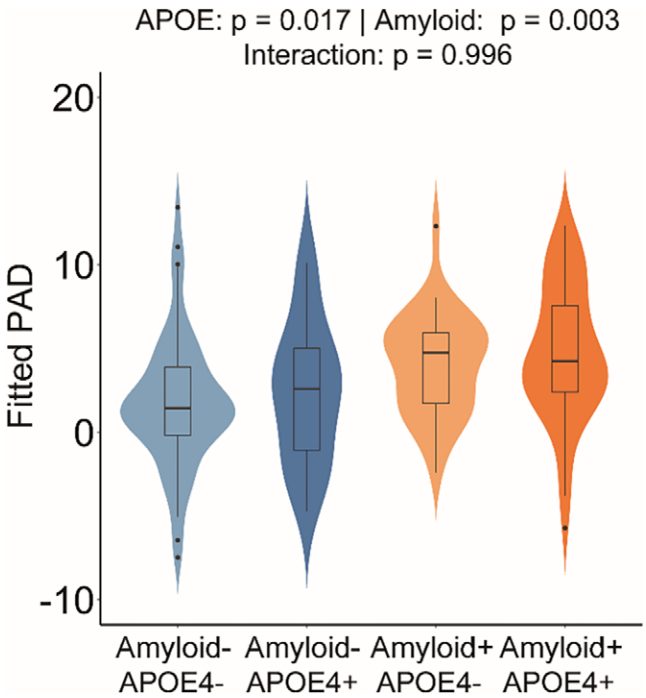

Figure 4: Violin plot shows effects of different Alzheimer disease risk factors on predicted age difference (PAD) in patients with amnestic mild cognitive impairment (aMCI). Main effects of apolipoprotein E (APOE) and amyloid status on PAD in patients with aMCI were statistically significant, whereas amyloid × APOE status interaction effect on PAD was not significant. There were 54 APOE $\varepsilon 4$ noncarriers with amyloid-negative (Amyloid−) status, 28 APOE $\varepsilon 4$ noncarriers with amyloid-positive (Amyloid+) status, 17 APOE $\varepsilon 4$ carriers with amyloid-negative (APOE4−) status, and 45 APOE $\varepsilon 4$ carriers with amyloid-positive (APOE4+) status.

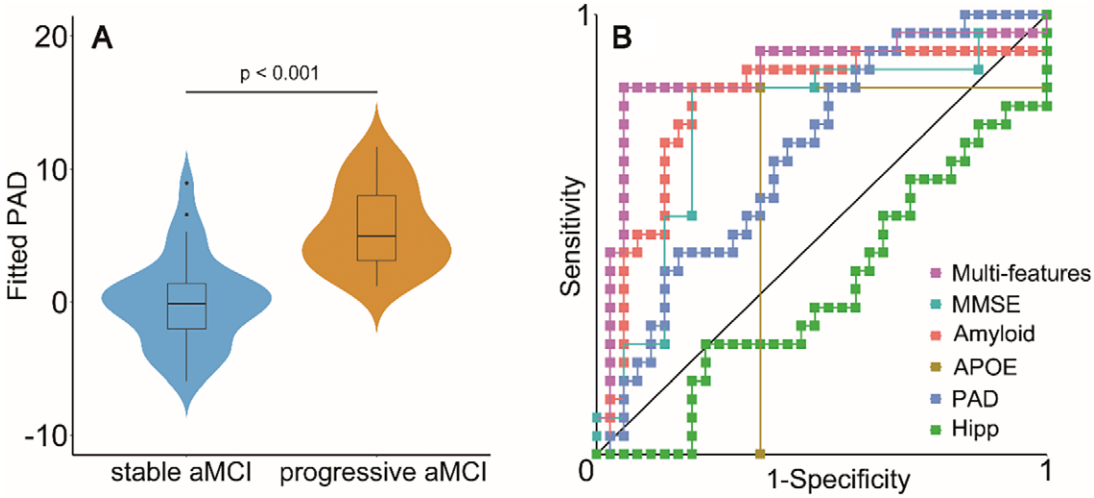

Figure 5: Clinical progression prediction with predicted age difference (PAD) in patients with amnestic mild cognitive impairment (aMCI). **(A)** Violin plot shows progressive aMCI group had larger PAD than stable aMCI group. **(B)** Graph shows PAD at baseline combined with Chinese version of Mini-Mental State Examination (MMSE) score, amyloid standardized uptake value ratio, and apolipoprotein E (APOE) allele status outperformed any single feature in discriminating progressive aMCI from stable aMCI. Hipp = hippocampal volume, Multi-features = PAD, MMSE, amyloid, and APOE allele status.

Table 6: Classification Performance between Stable aMCI and Progressive aMCI with Different Feature Sets

		Accuracy			Sensitivity			Specificity		
No.	Features	Value	*P* Value	95% CI	Value	*P* Value	95% CI	Value	*P* Value	95% CI
1	PAD, MMSE, Amyloid, APOE	0.877	.001	(0.792, 0.962)	0.833	.001	(0.684, 0.982)	0.909	.001	(0.811, 1)
2	MMSE, Amyloid, Hipp	0.842	.001	(0.747, 0.937)	0.792	.001	(0.630, 0.954)	0.879	.007	(0.768, 0.990)
3	PAD, MMSE, Amyloid, APOE, Hipp	0.842	.001	(0.747, 0.937)	0.792	.001	(0.630, 0.954)	0.879	.003	(0.768, 0.990)
4	MMSE, Amyloid	0.825	.001	(0.726, 0.924)	0.750	.004	(0.577, 0.923)	0.879	.133	(0.768, 0.990)
5	PAD, MMSE, Amyloid	0.825	.001	(0.726, 0.924)	0.792	.001	(0.630, 0.954)	0.849	.035	(0.727, 0.971)
6	PAD, MMSE, APOE	0.825	.001	(0.726, 0.924)	0.750	.001	(0.577, 0.923)	0.879	.030	(0.768, 0.990)
7	PAD, MMSE, Amyloid, Hipp	0.825	.001	(0.726, 0.924)	0.792	.001	(0.630, 0.954)	0.849	.006	(0.727, 0.971)
8	MMSE, Amyloid, APOE, Hipp	0.825	.001	(0.726, 0.924)	0.792	.001	(0.630, 0.954)	0.849	.010	(0.727, 0.971)
9	MMSE, Amyloid, APOE	0.807	.001	(0.705, 0.909)	0.750	.001	(0.577, 0.923)	0.849	.092	(0.727, 0.971)
10	Amyloid, APOE	0.790	.001	(0.684, 0.896)	0.750	.004	(0.577, 0.923)	0.818	.451	(0.686, 0.950)
11	PAD, MMSE	0.772	.001	(0.663, 0.881)	0.708	.001	(0.526, 0.890)	0.818	.323	(0.686, 0.950)
12	PAD, Amyloid	0.772	.001	(0.663, 0.881)	0.583	.023	(0.386, 0.780)	0.909	.025	(0.811, 1)
13	MMSE, APOE	0.772	.001	(0.663, 0.881)	0.708	.006	(0.526, 0.890)	0.818	.385	(0.686, 0.950)
14	PAD, MMSE, Hipp	0.754	.001	(0.642, 0.866)	0.708	.001	(0.526, 0.890)	0.788	.200	(0.649, 0.927)
15	Amyloid, APOE, Hipp	0.754	.001	(0.642, 0.866)	0.750	.001	(0.577, 0.923)	0.758	.397	(0.612, 0.904)
16	MMSE	0.719	.001	(0.602, 0.836)	0.542	.012	(0.343, 0.741)	0.849	.703	(0.727, 0.971)
17	Amyloid	0.719	.001	(0.602, 0.836)	0.500	.032	(0.300, 0.700)	0.879	.502	(0.768, 0.990)
18	APOE	0.719	.001	(0.602, 0.836)	0.833	.001	(0.684, 0.982)	0.636	.621	(0.472, 0.800)
19	PAD, APOE	0.719	.001	(0.602, 0.836)	0.792	.001	(0.630, 0.954)	0.667	.794	(0.506, 0.828)
20	MMSE, Hipp	0.719	.001	(0.602, 0.836)	0.625	.002	(0.431, 0.819)	0.788	.506	(0.649, 0.927)
21	Amyloid, Hipp	0.719	.001	(0.602, 0.836)	0.500	.032	(0.300, 0.700)	0.879	.072	(0.768, 0.990)
22	APOE, Hipp	0.702	.001	(0.583, 0.821)	0.792	.001	(0.630, 0.954)	0.636	.889	(0.472, 0.800)
23	PAD	0.649	.001	(0.525, 0.773)	0.458	.036	(0.259, 0.657)	0.788	.810	(0.649, 0.927)
24	PAD, Hipp	0.632	.001	(0.507, 0.757)	0.417	.069	(0.220, 0.614)	0.788	.459	(0.649, 0.927)
25	Hipp	0.456	.949	(0.327, 0.585)	0	.471	(0, 0)	0.788	.827	(0.649, 0.927)

Note.—APOE = apolipoprotein E, Hipp = hippocampal volume, MMSE = Mini-Mental State Examination, PAD = predicted age difference.

this aging process is accelerated in these individuals has not been precisely quantified.

Individual PADs in patients with aMCI were related to the severity of cognitive impairment, especially in memory, which was validated in both datasets, and the same relationship was not discovered in healthy controls. This evidence showed that brain age could explain individual differences of cognitive decline that were caused by AD pathologic characteristics rather than aging and that it has potential to be a quantitative measure of clinical progression in patients with aMCI. The result was also consistent with the concept that accelerated brain aging is the substrate of cognitive impairment (39). Moreover, we also found that PAD could capture cognitive impairments in attention that were typically influenced by AD in the BABRI dataset, which implied PAD might be a general marker of brain health. Furthermore, the significant correlation between PADs and MMSE scores indicated that PAD has potential as a fully automated criterion that could be used to assess the disease severity independent of typical aging in aMCI. Previous studies have demonstrated that PAD is related to the severity of disease within the whole spectrum of AD (9). However, whether PAD can quantify the degree of clinical progress in patients with aMCI, which is a critical stage to prevent or mitigate cognitive impairments, remained unclear before this study. Our results showed that PAD may have good potential for early diagnosis and monitoring response to treatment.

In aMCI, APOE $\varepsilon 4$ carriers had higher PADs than those of noncarriers. This finding suggests that the brains of APOE $\varepsilon 4$ carriers may age faster than noncarriers, which has been supported by longitudinal studies (40). Similarly, we found that in patients with aMCI, those with amyloid-positive disease also had higher PADs than those who were amyloid negative. These results suggest the brains of patients in different aMCI subgroups atrophy along various brain-aging trajectories, namely, more rapid progression to AD in aMCI groups with AD risk factors, such as APOE $\varepsilon 4$ and amyloid pathologic characteristics. These results also indicate that individual differences in brain aging in aMCI were modulated by multiple risk factors for AD, including APOE genotype and amyloid β deposition. In addition, the nonsignificant interaction effect showed that APOE genotype and amyloid β influence the brain-aging trajectory independently, which explains why there is no interaction between APOE $\varepsilon 4$ and cerebral amyloid β load in the context of cognitive function (41).

Patients with progressive aMCI had higher PADs compared with those with stable disease, which suggests that patients with progressive disease may have more severe brain degeneration and are in a later stage of the AD spectrum, which is consistent with the results of Löwe et al (15). In contrast to our findings, one study reported that the PAD could not distinguish stable aMCI from progressive aMCI (9). A possible explanation for this discrepancy is the fact that the brain age model by Beheshti et al (9) was not accurate enough (mean absolute error = 4.02, r = 0.68) to detect the subtle differences between the two aMCI groups. Moreover, the individual differences in brain-aging trajectories may explain the heterogeneous clinical progression of aMCI. More importantly, the classification results between stable and progressed aMCI indicate that combining PAD with more disease-specific markers will lead to further improvements in disease prediction. Compared with hippocampal volume, PADs might involve more comprehensive brain structure impairments; thus, the combination of the PAD, MMSE score, amyloid level, and APOE status may provide the highest performance. These results strongly suggest the potential of including PAD values for screening patients with aMCI, with the goal of identifying those at particularly high risk of progressing to AD as opposed to patients who will remain at a stable cognitive level.

A few other potential limitations of the study should also be noted. First, our model may not be precise enough to represent healthy brain-aging trajectories because we did not exclude older individuals who may have potential pathologic findings, such as small vessel ischemic disease, amyloid plaques, and τ neurofibrillary tangles. This means that our model may be affected by some neuropathologic aging, which limits its ability to detect some subtle pathologic findings. Therefore, future work should be done to build a more precise brain age prediction model that can be applied in clinical settings. Second, the proportion of the variance of cognition explained by PAD was low in patients with aMCI. This may be because we considered only structural degeneration in brain aging, whereas functional degeneration and vascular health are important for brain health and are associated with cognitive performance and the incidence of AD. Thus, multimodal imaging is needed for a more comprehensive brain age prediction model.

In conclusion, our study demonstrated that PAD could quantify individual deviations from the typical brain-aging trajectory in patients with aMCI and that this deviation was related to cognitive impairment, APOE genotype, amyloid β deposition, and clinical progression in patients with aMCI. In this process, we were able to leverage the developed algorithms for PAD quantification for assessment with the aforementioned clinical variables. Taken together, this study suggests that PAD has the potential to be developed into a computerized marker for early diagnosis of cognitive impairment and monitoring response to treatment.

Acknowledgments: The authors thank all of the volunteers and patients for their participation in the study and the anonymous reviewers for their insightful comments and suggestions.

Author contributions: Guarantors of integrity of entire study, W.H., X.L., J.Z., Y.C., N.S., Z.Z.; study concepts/study design or data acquisition or data analysis/interpretation, all authors; manuscript drafting or manuscript revision for important intellectual content, all authors; approval of final version of submitted manuscript, all authors; agrees to ensure any questions related to the work are appropriately resolved, all authors; literature research, W.H., X.L., K.X., J.Z., D.W., N.S., Z.Z.; clinical studies, W.W., J.Z., D.W., N.S.; experimental studies, X.L., H.L., J.Z., D.W., N.S., Z.Z.; statistical analysis, W.H., K.C., J.Z., Y.C., D.W., N.S.; and manuscript editing, W.H., X.L., H.L., K.C., J.Z., Y.C., D.W., N.S., Z.Z.

Disclosures of Conflicts of Interest: **W.H.** disclosed no relevant relationships. **X.L.** disclosed no relevant relationships. **H.L.** disclosed no relevant relationships. **W.W.** disclosed no relevant relationships. **K.C.** Activities related to the present article: disclosed no relevant relationships. Activities not related to the present article: has multiple grants from NIH/NIA supporting Alzheimer research but not related to this work; author is consultant for Green Valley Pharmaceutical (Shanghai, China); employee of Banner Alzheimer's Institute; institution has multiple NIH/NIA grants for AD research; adjunct professor with Beijing Normal U. Other relationships: involved in research from the Sixth People's hospital, Shanghai, China. **K.X.** disclosed no relevant relationships. **J.Z.** disclosed no relevant relationships. **Y.C.** disclosed no relevant relationships. **D.W.** disclosed no relevant relationships. **N.S.** disclosed no relevant relationships. **Z.Z.** disclosed no relevant relationships.

References

1. Petersen RC, Smith GE, Waring SC, Ivnik RJ, Tangalos EG, Kokmen E. Mild cognitive impairment: clinical characterization and outcome. Arch Neurol 1999;56(3):303–308 [Published correction appears in Arch Neurol 1999 Jun;56(6):760.].
2. Dickerson BC, Wolk DA; Alzheimer's Disease Neuroimaging Initiative. Dysexecutive versus amnesic phenotypes of very mild Alzheimer's disease are associated with distinct clinical, genetic and cortical thinning characteristics. J Neurol Neurosurg Psychiatry 2011;82(1):45–51.
3. Su F, Shu H, Ye Q, et al. Integration of Multilocus Genetic Risk into the Default Mode Network Longitudinal Trajectory during the Alzheimer's Disease Process. J Alzheimers Dis 2017;56(2):491–507.
4. deToledo-Morrell L, Stoub TR, Bulgakova M, et al. MRI-derived entorhinal volume is a good predictor of conversion from MCI to AD. Neurobiol Aging 2004;25(9):1197–1203.
5. Cole JH, Franke K. Predicting Age Using Neuroimaging: Innovative Brain Ageing Biomarkers. Trends Neurosci 2017;40(12):681–690.
6. Cole JH, Marioni RE, Harris SE, Deary IJ. Brain age and other bodily 'ages': implications for neuropsychiatry. Mol Psychiatry 2019;24(2):266–281.
7. Franke K, Luders E, May A, Wilke M, Gaser C. Brain maturation: predicting individual BrainAGE in children and adolescents using structural MRI. Neuroimage 2012;63(3):1305–1312.
8. Franke K, Ziegler G, Klöppel S, Gaser C; Alzheimer's Disease Neuroimaging Initiative. Estimating the age of healthy subjects from T1-weighted MRI scans using kernel methods: exploring the influence of various parameters. Neuroimage 2010;50(3):883–892.
9. Beheshti I, Maikusa N, Matsuda H. The association between "Brain-Age Score" (BAS) and traditional neuropsychological screening tools in Alzheimer's disease. Brain Behav 2018;8(8):e01020.
10. Cole JH, Leech R, Sharp DJ; Alzheimer's Disease Neuroimaging Initiative. Prediction of brain age suggests accelerated atrophy after traumatic brain injury. Ann Neurol 2015;77(4):571–581.
11. Cole JH, Underwood J, Caan MW, et al. Increased brain-predicted aging in treated HIV disease. Neurology 2017;88(14):1349–1357 [Published correction appears in Neurology 2017;89(15):1652.].
12. Schnack HG, van Haren NE, Nieuwenhuis M, Hulshoff Pol HE, Cahn W, Kahn RS. Accelerated Brain Aging in Schizophrenia: A Longitudinal Pattern Recognition Study. Am J Psychiatry 2016;173(6):607–616.
13. Gaser C, Franke K, Klöppel S, Koutsouleris N, Sauer H; Alzheimer's Disease Neuroimaging Initiative. BrainAGE in Mild Cognitive Impaired Patients: Predicting the Conversion to Alzheimer's Disease. PLoS One 2013;8(6):e67346.
14. Liem F, Varoquaux G, Kynast J, et al. Predicting brain-age from multimodal imaging data captures cognitive impairment. Neuroimage 2017;148:179–188.
15. Löwe LC, Gaser C, Franke K; Alzheimer's Disease Neuroimaging Initiative. The Effect of the APOE Genotype on Individual BrainAGE in Normal Aging, Mild Cognitive Impairment, and Alzheimer's Disease. PLoS One 2016;11(7):e0157514.
16. Wang J, Knol MJ, Tiulpin A, et al. Gray Matter Age Prediction as a Biomarker for Risk of Dementia. Proc Natl Acad Sci U S A 2019;116(42):21213–21218.
17. Ly M, Yu GZ, Karim HT, et al. Improving brain age prediction models: incorporation of amyloid status in Alzheimer's disease. Neurobiol Aging 2020;87:44–48.
18. Nho K, Risacher SL, Crane PK, et al. Voxel and surface-based topography of memory and executive deficits in mild cognitive impairment and Alzheimer's disease. Brain Imaging Behav 2012;6(4):551–567.
19. Li X, Wang Y, Wang W, et al. Age-Related Decline in the Topological Efficiency of the Brain Structural Connectome and Cognitive Aging. Cereb Cortex 2020;30(8):4651–4661.
20. Petersen RC. Mild cognitive impairment as a diagnostic entity. J Intern Med 2004;256(3):183–194.
21. Jack CR Jr, Bernstein MA, Fox NC, et al. The Alzheimer's Disease Neuroimaging Initiative (ADNI): MRI methods. J Magn Reson Imaging 2008;27(4):685–691.
22. Tzourio-Mazoyer N, Landeau B, Papathanassiou D, et al. Automated anatomical labeling of activations in SPM using a macroscopic anatomical parcellation of the MNI MRI single-subject brain. Neuroimage 2002;15(1):273–289.
23. Jack CR Jr, Wiste HJ, Therneau TM, et al. Associations of Amyloid, Tau, and Neurodegeneration Biomarker Profiles With Rates of Memory Decline Among Individuals Without Dementia. JAMA 2019;321(23):2316–2325.
24. Jack CR Jr, Wiste HJ, Weigand SD, et al. Defining imaging biomarker cut points for brain aging and Alzheimer's disease. Alzheimers Dement 2017;13(3):205–216.
25. Kantarci K, Lowe VJ, Chen Q, et al. β-Amyloid PET and neuropathology in dementia with Lewy bodies. Neurology 2020;94(3):e282–e291.
26. Mielke MM, Hagen CE, Xu J, et al. Plasma phospho-tau181 increases with Alzheimer's disease clinical severity and is associated with tau- and amyloid-positron emission tomography. Alzheimers Dement 2018;14(8):989–997.
27. Barretina J, Caponigro G, Stransky N, et al. The Cancer Cell Line Encyclopedia enables predictive modelling of anticancer drug sensitivity. Nature 2012;483(7391):603–607 [Published correction appears in Nature 2012;492(7428):290. Published addendum appears in Nature 2019;565(7738):E5–E6.].
28. Cui Z, Su M, Li L, Shu H, Gong G. Individualized Prediction of Reading Comprehension Ability Using Gray Matter Volume. Cereb Cortex 2018;28(5):1656–1672.
29. Cole JH, Poudel RPK, Tsagkrasoulis D, et al. Predicting brain age with deep learning from raw imaging data results in a reliable and heritable biomarker. Neuroimage 2017;163:115–124.
30. Scheinost D, Noble S, Horien C, et al. Ten simple rules for predictive modeling of individual differences in neuroimaging. Neuroimage 2019;193:35–45.
31. Johnson JW, Lebreton JM. History and Use of Relative Importance Indices in Organizational Research. Organ Res Methods 2016;7(3):238–257.
32. Cole JH, Annus T, Wilson LR, et al. Brain-predicted age in Down syndrome is associated with beta amyloid deposition and cognitive decline. Neurobiol Aging 2017;56:41–49.
33. Crivello F, Tzourio-Mazoyer N, Tzourio C, Mazoyer B. Longitudinal assessment of global and regional rate of grey matter atrophy in 1,172 healthy older adults: modulation by sex and age. PLoS One 2014;9(12):e114478.
34. Curiati PK, Tamashiro JH, Squarzoni P, et al. Brain structural variability due to aging and gender in cognitively healthy Elders: results from the Sao Paulo Ageing and Health study. AJNR Am J Neuroradiol 2009;30(10):1850–1856.
35. Tisserand DJ, van Boxtel MP, Pruessner JC, Hofman P, Evans AC, Jolles J. A voxel-based morphometric study to determine individual differences in gray matter density associated with age and cognitive change over time. Cereb Cortex 2004;14(9):966–973.
36. Chételat G, Desgranges B, De La Sayette V, Viader F, Eustache F, Baron JC. Mapping gray matter loss with voxel-based morphometry in mild cognitive impairment. Neuroreport 2002;13(15):1939–1943.
37. Jack CR Jr, Bernstein MA, Borowski BJ, et al. Update on the magnetic resonance imaging core of the Alzheimer's disease neuroimaging initiative. Alzheimers Dement 2010;6(3):212–220.
38. Driscoll I, Davatzikos C, An Y, et al. Longitudinal pattern of regional brain volume change differentiates normal aging from MCI. Neurology 2009;72(22):1906–1913.
39. Smits LL, Tijms BM, Benedictus MR, et al. Regional atrophy is associated with impairment in distinct cognitive domains in Alzheimer's disease. Alzheimers Dement 2014;10(5 Suppl):S299–S305.
40. Aguilar C, Muehlboeck JS, Mecocci P, et al. Application of a MRI based index to longitudinal atrophy change in Alzheimer disease, mild cognitive impairment and healthy older individuals in the AddNeuroMed cohort. Front Aging Neurosci 2014;6:145.
41. Lim YY, Ellis KA, Pietrzak RH, et al. Stronger effect of amyloid load than APOE genotype on cognitive decline in healthy older adults. Neurology 2012;79(16):1645–1652.